Diagnosis of pseudoprogression following lomustine-temozolomide chemoradiation in newly diagnosed glioblastoma patients using FET PET

Jan-Michael Werner¹, Johannes Weller², Garry Ceccon¹, Christina Schaub², Caroline Tscherpel¹, Philipp Lohmann^{3,4}, Elena K. Bauer¹, Niklas Schäfer², Gabriele Stoffels³, Christian Baues⁵, Eren Celik⁵, Simone Marnitz^{5,6}, Christoph Kabbasch⁷, Gerrit H. Gielen⁸, Gereon R. Fink^{1,3}, Karl-Josef Langen^{3,6,9}, Ulrich Herrlinger^{2,6}, and Norbert Galldiks^{1,3,6}

¹Dept. of Neurology, Faculty of Medicine and University Hospital Cologne, University of Cologne, Cologne, Germany

²Division of Clinical Neurooncology, Department of Neurology, University Hospital Bonn, Bonn, Germany

³Inst. of Neuroscience and Medicine (INM-3, -4), Research Center Juelich, Juelich, Germany

⁴Dept. of Stereotaxy and Functional Neurosurgery, Faculty of Medicine and University Hospital Cologne, University of Cologne, Cologne, Germany

⁵Dept. of Radiation Oncology and Cyberknife Center, Faculty of Medicine and University Hospital Cologne, Cologne, Germany

⁶Center for Integrated Oncology (CIO), Universities of Aachen, Bonn, Cologne, and Duesseldorf, Germany

⁷Dept. of Neuroradiology, Faculty of Medicine and University Hospital Cologne, University of Cologne, Cologne, Germany

⁸Inst. of Neuropathology, University Hospital Bonn, Bonn, Germany ⁹Dept. of Nuclear Medicine, University Hospital Aachen, Aachen, Germany

Running title:

FET PET and lomustine-temozolomide pseudoprogression

To be submitted to Clinical Cancer Research

Correspondence

Jan-Michael Werner, MD

Dept. of Neurology, University Hospital Cologne, Kerpener St. 62, 50937 Cologne,

Germany

Phone: +49-221-478-84695, FAX: +49-221-478-77084

Email: jan-michael.werner@uk-koeln.de

Disclosure of Potential Conflicts of Interest

UH has received lecture and/or advisory board honoraria from Medac, Novartis, Daichii-Sankyo, Noxxon, AbbVie, Bayer, Janssen, and Karyopharm. The other authors disclosed no potential conflicts of interest.

Word count

Manuscript body: 3,784

Abstract: 250

References: 1,748

ABSTRACT

Background: The CeTeG/NOA-09 phase-III trial demonstrated a significant survival benefit of lomustine-temozolomide chemoradiation in newly diagnosed glioblastoma patients with methylated O⁶-methylguanine-DNA methyltransferase promoter. Following lomustine-temozolomide chemoradiation, late and prolonged pseudoprogression may occur. We here evaluated the value of amino acid PET using O-(2-[¹⁸F]fluoroethyl)-L-tyrosine (FET) for differentiating pseudoprogression from tumor progression.

Methods: We retrospectively identified patients (i) who were treated off-study according to the CeTeG/NOA-09 protocol, (ii) had equivocal MRI findings after radiotherapy, and (iii) underwent additional FET-PET imaging for diagnostic evaluation (number of scans, 1-3). Maximum and mean tumor-to-brain ratios (TBR_{max}, TBR_{mean}) and dynamic FET uptake parameters (e.g., time-to-peak) were calculated. In patients with more than one FET-PET scan, relative changes of TBR values were evaluated, i.e., an increase or decrease of >10% compared to the reference scan was considered as tumor progression or pseudoprogression. Diagnostic performances were evaluated using receiver operating characteristic curve analyses and Fisher's exact test. Diagnoses were confirmed histologically or clinicoradiologically.

Results: We identified 23 patients with 32 FET-PET scans. Within 5-25 weeks after radiotherapy (median time, 9 weeks), pseudoprogression occurred in 11 patients (48%). The parameter TBR_{mean} calculated from the FET-PET performed 10 ± 7 days after the equivocal MRI showed the highest accuracy (87%) to identify pseudoprogression (threshold, <1.95; P=0.029). The integration of relative changes

of TBR_{mean} further improved the accuracy (91%; P<0.001). Moreover, the combination of static and dynamic parameters increased the specificity to 100% (P=0.005).

Conclusions: The data suggest that FET-PET parameters are of significant clinical value to diagnose pseudoprogression related to lomustine-temozolomide chemoradiation.

KEYWORDS

treatment-related changes; treatment monitoring; lomustine; temozolomide; chemoradiation

STATEMENT OF TRANSLATIONAL RELEVANCE

The prospective CeTeG/NOA-09 phase-III trial recently demonstrated a significant overall survival benefit of temozolomide-lomustine chemoradiation as first-line therapy in glioblastoma patients with methylated MGMT promoter. Notably, following lomustine-temozolomide chemoradiation, late and prolonged pseudoprogression may occur, even three months after radiotherapy completion. Furthermore, several studies suggested that pseudoprogression occurs more frequently in patients with methylated MGMT promoter. Therefore, the decision to discontinue temozolomidelomustine chemotherapy in patients with equivocal or progressive findings on conventional MRI after radiotherapy should be as reliable as possible because the specificity of this technique for delineating neoplastic tissue is low. To overcome this challenging situation, it has repeatedly been suggested that amino acid PET is a powerful diagnostic tool for differentiating pseudoprogression from actual tumor progression. The present study provides evidence that static and dynamic FET PET is of clinical value for detecting pseudoprogression following temozolomide-lomustine chemoradiation and helps to prevent premature discontinuation of an effective treatment.

INTRODUCTION

Glioblastoma is a devastating disease with median overall survival times in unselected study populations of around 15-20 months (1,2). Importantly, the subgroup of glioblastoma patients with a methylated O⁶-methylguanine-DNA methyltransferase (MGMT) promoter treated with temozolomide chemoradiation has a better prognosis with median survival times beyond 20 months (3). The prolonged survival is mainly due to the susceptibility of the MGMT promotor methylated glioblastoma cells to alkylating chemotherapy (4). The prospective CeTeG/NOA-09 phase-III trial recently demonstrated that the median overall survival can be further prolonged to approximately 48 months by lomustine-temozolomide chemoradiation as first-line therapy in glioblastoma patients with methylated MGMT promoter (5).

However, chemoradiation with intensified alkylating chemotherapy using lomustine and temozolomide applied according to the CeTeG/NOA-09 trial protocol may cause prolonged and/or delayed pseudoprogression (6). For example, Stuplich and colleagues described that this phenomenon occurs substantially later than 12 weeks after radiotherapy (onset, 17-50 weeks) (6). In contrast, pseudoprogression following standard chemoradiation with temozolomide alone occurs earlier, typically within the first 12 weeks after radiotherapy completion (7-9). Therefore, this time-dependent definition has been incorporated into the criteria defined by the Response Assessment in Neuro-Oncology Working Group (RANO criteria) (7).

Furthermore, an earlier study reported an increased pseudoprogression rate in glioma patients with methylated MGMT promoter (9). Most probably due to standardizing the assessment of response, tumor progression, and pseudoprogression using strict algorithms in subsequent phase-III clinical trials

(5,10), this association could no longer be observed. On the other hand, one of the most extensive studies with more than 250 glioblastoma patients treated with temozolomide chemoradiation reported a 3.5-fold greater probability to develop pseudoprogression if a MGMT promoter methylation is present (11). Thus, the effect of an MGMT promoter methylation on the development of pseudoprogression cannot be neglected.

Neurooncological centers, especially in Europe, are increasingly offering lomustine-temozolomide chemoradiation due to its survival-prolonging effects, which may also provoke a higher pseudoprogression rate. Importantly, this can lead to an erroneously premature termination of lomustine-temozolomide chemotherapy with a potential negative prognostic impact and the misinterpretation of response using conventional MRI. Such an incorrect diagnosis may also lead to an inadequate patient inclusion in clinical trials, eventually resulting in misleading data about the applied treatment for (falsely assumed) progressive disease, thereby overestimating efficacy.

Contrast-enhanced conventional MRI is the cornerstone of brain tumor imaging, but this technique suffers from low specificity despite excellent spatial resolution (12-14). The differentiation of treatment-related changes from actual tumor progression represents a major problem not only after chemoradiation with alkylating agents but also with other treatment options currently used in brain tumor patients (e.g., antiangiogenic therapy, checkpoint inhibitor immunotherapy, or targeted therapy, especially in combination with radiotherapy) (15-17).

To overcome the limitations of conventional MRI, diagnostic tools with higher accuracy are necessary. In recent years, it has repeatedly been shown that in glioma patients, PET using the radiolabeled amino acid *O*-(2-[¹⁸F]fluoroethyl)-L-tyrosine (FET) offers high diagnostic accuracy for differentiating pseudoprogression from actual tumor progression (18-23). Additionally, the high clinical value of amino acid PET for identifying treatment-related changes in patients with primary and secondary brain tumors has been highlighted by the Response Assessment in Neuro-Oncology (RANO) Working Group (24,25).

FET is not significantly incorporated into any metabolic pathway and has no relevant participation in protein synthesis and is transported via specific amino acid transporters especially by the system of L-type amino acid transporters (LAT), particularly the subtypes LAT1 and LAT2 (26). An experimental study suggested that the overexpression of LAT1 strongly facilitates the influx of FET. On the other hand, FET turned out to be a poor efflux substrate of LAT1. Thus, this asymmetry may cause the intracellular entrapment of FET (27).

We evaluated the diagnostic performance of static and dynamic FET PET parameters for differentiating pseudoprogression from actual tumor progression in glioblastoma patients with methylated MGMT promoter treated off-study with lomustine-temozolomide chemoradiation according to the CeTeG/NOA-09 protocol.

PATIENTS AND METHODS

Patients

From 2018-2020, we retrospectively identified patients who (i) were treated off-study according to the CeTeG/NOA-09 protocol (5), (ii) had equivocal or progressive MRI findings after radiotherapy inside the radiation field (i.e., within the 80% isodose), and (iii) underwent additional FET PET imaging for diagnostic evaluation (number of scans, 1-3).

According to the CeTeG/NOA-09 protocol (5), the patients underwent external fractionated radiotherapy (60 Gy, 30 fractions over six weeks) after resection or biopsy. In addition to radiotherapy, the patients received up to six cycles of lomustine (100 mg/m² on day 1) plus temozolomide (100-200 mg/m² per day on days 2-6 of the 6-week course). The first cycle of lomustine-temozolomide chemotherapy started in the first week of radiotherapy.

The local ethics committees approved the retrospective analysis of neuroimaging data. There was no conflict with the Declaration of Helsinki. Before PET imaging, all patients had given written informed consent for the PET investigation and the use of the data for scientific purposes.

Diagnosis of Pseudoprogression or Tumor Progression

If available, neuropathological analysis after biopsy or resection at the time of progression was used to diagnose pseudoprogression or tumor progression. In those cases, the presence of viable tumor tissue confirmed tumor progression. On the other hand, pseudoprogression was considered if histology predominantly showed features

typically associated with treatment effects such as bland necrosis, fibrosis, gliosis, edema, demyelination, and vascular hyalinization (28).

In cases without neuropathological confirmation, pseudoprogression was assumed if after an initial MRI with equivocal or progressive lesion(s) according to RANO criteria (7) (i) MRI findings remained stable or subsequently improved during follow-up examinations performed every 8-12 weeks, (ii) the clinical status remained stable or improved again after initial deterioration during follow-up examinations performed every 8-12 weeks, and (iii) the treatment was not changed during the following 6 months. This definition was modified from Young and colleagues (29). Tumor progression was diagnosed if MRI changes, or clinical deterioration prompted a treatment change.

Conventional MR Imaging

Following the International Standardized Brain Tumor Imaging Protocol (BTIP) (30), MR imaging was performed using a 1.5 T or 3.0 T scanner before and after administration of a gadolinium-based contrast agent (0.1 mmol/kg body weight). The sequence protocol comprised at least 3D isovoxel T1-weighted, 2D T2-weighted, and 2D fluid-attenuated inversion recovery-weighted (FLAIR) sequences.

FET PET Imaging

As described previously, the amino acid FET was produced via nucleophilic ¹⁸F-fluorination with a radiochemical purity of greater than 98%, specific radioactivity greater than 200 GBq/µmol, and a radiochemical yield of about 60% (19,31). According to international guidelines for brain tumor imaging using radiolabeled amino acid analogs (32), all patients fasted for at least 4 h before the PET

measurements. All patients underwent a dynamic PET scan from 0 to 50 minutes post-injection of 3 MBq of FET per kg of body weight. PET imaging was performed either on an ECAT Exact HR+ PET scanner (n=14 patients) in 3-dimensional mode (Siemens, Erlangen, Germany) (axial field-of-view, 15.5 cm; spatial resolution, 6 mm) or simultaneously with 3T MR imaging using a BrainPET insert (n=9 patients) (Siemens, Erlangen, Germany). The BrainPET is a compact cylinder that fits in the Magnetom Trio MR scanner (axial field of view, 19.2 cm; spatial resolution, 3 mm) (33). Iterative reconstruction parameters were 16 subsets, 6 iterations using the OSEM algorithm for the ECAT HR+ PET scanner, and two subsets, 32 iterations using the OP-OSEM algorithm for the BrainPET. Data were corrected for random, scattered coincidences, dead time, and motion for both systems. Attenuation correction for the ECAT HR+ PET data was based on a transmission scan, and for the BrainPET data on a template-based approach (33). The reconstructed dynamic data set consisted of 16 time frames (5 x 1 minutes; 5 x 3 minutes; 6 x 5 minutes) for both scanners.

To optimize comparability of the results related to the influence of the two different PET scanners, reconstruction parameters, and post-processing steps, a 2.5 mm 3D Gaussian filter was applied to the BrainPET data before further processing as described previously (19). In phantom experiments using spheres of different sizes to simulate lesions, this filter kernel demonstrated the best comparability between PET data obtained from the ECAT HR+ PET and the BrainPET scanner (34).

FET PET Data Analysis

Static FET PET data analysis was based on summed PET images over 20-40 minutes post-injection. The tumor area on FET PET scans was determined by a two-

dimensional auto-contouring process using a tumor-to-brain ratio (TBR) of 1.6 or more as described previously (19,35,36). Maximum and mean tumor-to-brain ratios (TBR $_{max}$, TBR $_{mean}$) were calculated by dividing the maximum and mean standardized uptake value (SUV) of the tumor regions of interest by the mean SUV of healthy brain tissue.

As described previously (19,37), time-activity curves (TACs) of the mean FET uptake in the tumor were generated by applying a spherical volume-of-interest (VOI) with a volume of 2 mL centered on the voxel with the maximum tumor uptake to the entire dynamic dataset. A reference TAC was generated by placing a reference ROI in the unaffected brain tissue as reported (37). For TAC evaluation, the time-to-peak (TTP; time in minutes from the beginning of the dynamic acquisition up to the maximum SUV of the lesion) was determined. In cases with steadily increasing FET uptake without identifiable peak, we defined the end of the dynamic PET acquisition as TTP. Furthermore, the TAC slope in the late phase of FET uptake was assessed by fitting a linear regression line to the late phase of the curve (20-50 minutes post-injection). The slope was expressed as the change of the SUV per hour. This procedure allows for a more objective evaluation of kinetic data than an assignment of TACs to earlier reported patterns of FET uptake during dynamic acquisition (37).

Relative Changes of FET Uptake in Comparison to the Reference FET PET

In addition to evaluating a single FET PET scan corresponding to the suspicious MRI, the diagnostic value of relative TBR_{mean} changes was also evaluated in patients with more than one FET PET scan. A previous study has suggested that a decrease of the TBR_{mean} of 10% or more is of value to diagnose pseudoprogression in glioblastoma patients treated with standard temozolomide chemoradiation (38).

Accordingly, in patients with a reduction of TBR_{mean} of 10% or more than the reference FET PET scan without clinical deterioration, pseudoprogression was considered. Analogously, tumor progression was considered in case of an increase of $TBR_{mean} > 10\%$ compared to the reference FET PET scan.

Neuropathological Tumor Classification and Analysis of Molecular Markers

As described previously (39), all tumors were neuropathologically classified according to the WHO Classification of Tumors of the Central Nervous System of 2016 (40). For molecular biomarker analysis, tumor DNA was extracted from formalin-fixed and paraffin-embedded tissue samples with a histologically estimated tumor cell content of 80% or more. For assessment of the IDH mutation the presence of an IDH1-R132H mutation was evaluated by immunohistochemistry using a mutation-specific antibody in a standard immunohistochemical staining procedure as reported before (39,41,42). When immunostaining for IDH1-R132H remained negative, the mutational hot-spots at codon 132 of IDH1 and codon 172 of IDH2 were directly sequenced, as reported 1p/19q co-deletion status was determined by PCR-based (42,43). The O⁶-methylguanine-DNAmicrosatellite analysis as reported (44).The methyltransferase (MGMT) promoter methylation status was assessed by methylation-specific PCR as described elsewhere (43).

Statistical Evaluation

Descriptive statistics are provided as mean and standard deviation or median and range. For intergroup comparison, the Student t-test for independent samples was used when variables were normally distributed, and the Mann-Whitney-U test if variables were not normally distributed. Receiver operating characteristic (ROC)

curve analyses were performed to define the decision cut-off values for static and dynamic FET PET parameters using the neuropathological confirmation or clinicoradiological course as reference. The decision cut-off was considered optimal when the product of paired values for sensitivity and specificity reached its maximum. Moreover, the area under the ROC curve (AUC), its standard error, and level of significance were determined to measure the test's diagnostic quality. The Fisher exact test for 2×2 contingency tables was used to evaluate the diagnostic performance of FET PET parameters. *P*-values of 0.05 or less were considered significant. Statistical analyses were performed using GraphPad Prism (Release 8.4.3, GraphPad Software Inc., La Jolla, CA, USA).

RESULTS

Patients

According to our search criteria, we identified 23 adult patients (mean age, 58 ± 9 years; age range, 38-71 years; 10 females) with 32 FET PET scans and neuropathologically confirmed IDH-wildtype glioblastoma and methylated MGMT promoter. In addition, 7 patients were identified who underwent dynamic FET-PET imaging before initiating lomustine-temozolomide chemoradiation. Another patient underwent additional dynamic FET PET imaging before the initiation of lomustine-temozolomide chemoradiation and 7 weeks after the suspicious MRI.

After resection (n=12 complete resections, and n=7 partial resections) or stereotactic biopsy (n=4), all patients underwent external fractionated radiotherapy (60 Gy) plus lomustine-temozolomide chemotherapy according to the CeTeG/NOA-09 trial (5).

After radiotherapy completion, all patients exhibited equivocal MRI findings suspicious for tumor progression. Fifteen patients (65%) had a new contrast-enhancing lesion (n=9) or an enlargement of a preexisting contrast-enhancing lesion of at least 25% (n=6) according to the RANO criteria (7). Four patients had an enlargement of a preexisting contrast-enhancing lesion of less than 25%, and one patient had a new contrast-enhancing lesion with a maximum diameter smaller than 10 mm. Three patients had a signal increase of the perifocal hyperintensity on the T2- or FLAIR-weighted MRI of 15% or more (45). Patients' characteristics and MRI findings are listed in Table 1.

The mean time between completion of radiotherapy and the MRI suspicious for tumor progression was 14 ± 9 weeks (median time, 10 weeks; range, 5-34 weeks). All

patients underwent dynamic FET PET imaging to differentiate between pseudoprogression and actual tumor progression after a mean time of 10 ± 7 days (median time, 11 days; range, 0-26 days).

Pseudoprogression and Tumor Progression

In 11 of 23 patients (48%), pseudoprogression was diagnosed within 5-25 weeks after radiotherapy completion (median time, 9 weeks). In 9 patients, a stable clinical status combined with stable or improved MRI findings during a follow-up of more than 6 months (median follow-up, 12 months; range, 6-31 months) without treatment change confirmed pseudoprogression. In 7 of these 9 patients, the median time between pseudoprogression onset and the beginning of the improvement of MRI findings was 34 weeks (range, 26-99 weeks). One patient example is presented in Figure 1. In two patients, the neuropathological tissue examination of the suspicious lesion revealed no viable tumor cells, and reactive tissue changes confirmed pseudoprogression. One patient example is presented in Figure 2.

Tumor progression was confirmed in 12 of 23 patients (52%). In 8 patients, tumor progression was diagnosed clinicoradiologically (median follow-up, 2 months; range, 0-5 months). In the remaining 4 patients, the obtained neuropathological samples yielded predominantly viable tumor cells. A summary of results is provided in Table 2.

The median number of applied lomustine-temozolomide chemotherapy cycles before the occurrence of equivocal or progressive findings on MRI was 3 (range, 2-6 cycles). In patients with pseudoprogression or actual tumor progression, there were no significant differences in terms of age (57 \pm 9 vs. 59 \pm 10 years; P = 0.631) or the

extent of resection (complete resection rate in patients with pseudoprogression, 55%; complete resection rate in patients with actual tumor progression, 50%).

Diagnostic Performance of Conventional MRI

The diagnostic performance of conventional MRI based on RANO criteria (7) for the identification of pseudoprogression did not reach significance (accuracy, 58%; sensitivity, 30%; specificity, 79%; P = 0.665).

Static and Dynamic FET PET Parameters

The static FET uptake parameters TBR_{mean} and TBR_{max} were significantly lower in patients with pseudoprogression compared to patients with actual tumor progression (TBR_{mean}, 1.9 ± 0.2 vs. 2.1 ± 0.2 ; P = 0.023, and TBR_{max}, 2.8 ± 0.6 vs. 3.2 ± 0.5 ; P = 0.045). The dynamic PET parameter TTP was significantly higher in patients with pseudoprogression than with actual tumor progression (36.6 ± 8.3 vs. 24.8 ± 9.4 minutes; P = 0.005). Regarding the dynamic parameter slope, group comparison did not reach significance (P > 0.05). Results are summarized in Table 2.

Results of ROC Analyses

ROC analysis revealed that the optimal cut-off value of TBR_{mean} for the differentiation of pseudoprogression from actual tumor progression was 1.95 (sensitivity, 82%; specificity, 92%; accuracy 87%; AUC, 0.77 \pm 0.12; P=0.029). The corresponding TBR_{max} cut-off value was 2.85 (sensitivity, 64%; specificity, 92%; accuracy 78%; AUC, 0.75 \pm 0.11; P=0.046). Regarding the dynamic parameter TTP, ROC analysis revealed an optimal cut-off value of 35 minutes (sensitivity, 64%; specificity, 83%; accuracy 74%; AUC 0.82 \pm 0.09; P=0.010). The dynamic parameter slope yielded no statistically significant results.

Furthermore, the combination of TBR_{mean} with TTP increased both the specificity and positive predictive value to 100% for the detection of pseudoprogression (sensitivity, 55%; accuracy 78%; P = 0.005). An overview of the results is provided in Table 3.

Identification of Pseudoprogression with Relative Changes of FET Uptake

Relative changes of TBRs calculated from additional FET PET scans (n=9) of 8 patients provided additional diagnostic information. In 5 of these 8 patients, relative FET-uptake changes (i.e., > 10% decrease or increase of TBRs) enabled the diagnosis of pseudoprogression or tumor progression in 3 and 2 patients, respectively. The integration of relative TBR_{mean} changes yielded an improved diagnostic accuracy of 91% for identifying pseudoprogression (sensitivity, 91%; specificity, 92%; P < 0.001). The relative change of TBR_{max} did not improve diagnostic accuracy.

DISCUSSION

The main finding of the present study is that FET PET-derived imaging parameters seem to be of significant clinical value for detecting pseudoprogression in newly diagnosed IDH-wildtype glioblastoma with methylated MGMT promoter treated with lomustine-temozolomide chemoradiation. Consequently, suspicious MRI findings during that treatment regimen should be critically evaluated.

As described previously, FET PET-derived parameters show a high diagnostic accuracy for detecting treatment-related changes such as pseudoprogression or radiation necrosis following chemoradiation with standard alkylating agents (i.e., predominantly temozolomide) (18-20,22,37). The present results extend these findings, suggesting that both static and dynamic FET PET parameters are also of clinical value for detecting pseudoprogression related to lomustine-temozolomide chemoradiation. Regarding static parameters, the herein reported threshold of 1.95 for TBR_{mean} and the resulting high diagnostic accuracy are following earlier studies (18,19,46).

Furthermore, and in line with previous studies (19,37,46), we observed that dynamic FET parameters also have an additional diagnostic value for pseudoprogression detection. As outlined above, it is assumed that the different FET uptake kinetics is caused by a differential asymmetry of influx and efflux of FET in progressive tumor and pseudoprogression. In particular, the combination of static and dynamic FET PET parameters increased both the specificity and positive predictive value to 100%. Generally, conventional contrast-enhanced MRI provides high sensitivity, but its specificity for diagnosing treatment-related changes is limited (12). However, especially a high specificity is essential for the correct detection of

pseudoprogression and can be improved by static and dynamic FET PET parameter combinations.

Finally, in addition to FET PET parameter combinations, our study also highlights the value of relative changes of metabolic activity using serial FET PET imaging for diagnosing pseudoprogression. As observed in an earlier study (38), a reduction of TBR_{mean} of more than 10% was also associated with improved diagnostic accuracy for pseudoprogression.

For the management of patients with glioblastoma, another important issue is the onset of pseudoprogression following lomustine-temozolomide chemoradiation. In the majority of patients, we observed the onset of pseudoprogression within the first 12 weeks after radiotherapy completion. Notwithstanding, our study, pseudoprogression was diagnosed in two patients beyond the 12-week time window, indicating that pseudoprogression may also occur delayed. This observation is in line with the results of a study by Stuplich and colleagues. In that study, late and prolonged pseudoprogression was observed in 3 of 8 patients treated with lomustinetemozolomide chemoradiation, and the pseudoprogression onset was between 19-50 weeks after radiotherapy completion (6). Furthermore, the colleagues reported a slow improvement of contrast-enhancing lesions within 41-97 weeks, indicating prolonged pseudoprogression. In a more recent study, in two glioblastoma patients undergoing lomustine-temozolomide chemoradiation, late pseudoprogression occurred 18-24 weeks after radiotherapy completion (20). However, information on the improvement of contrast-enhancing lesions was not reported in all patients. In the present study, the latest pseudoprogression onset was 25 weeks after radiotherapy, and the most extended time interval between pseudoprogression onset and improvement of MRI findings was 99 weeks.

Following standard chemoradiation with temozolomide in patients with glioblastoma, previous studies suggested that pseudoprogression occurs most frequently within the first 12 weeks after chemoradiation completion (9,11,47-49). In contrast, the rate of late pseudoprogression beyond the 12-week window following standard temozolomide-based chemoradiation is relatively low (< 5%) and observed in single cases only (47,50-52). However, it is unclear why pseudoprogression was late or prolonged beyond the 12-week cut-off after radiotherapy. A possible explanation may be the long-lasting effects of lomustine (53). For example, Peyre and colleagues observed in 60% of 21 glioma patients treated with lomustine, procarbazine, and vincristine that a prolonged response can be detected more than two years after treatment discontinuation (median period, 2.7 years) (53). Accordingly, these long-lasting effects of nitrosoureas such as lomustine may also be responsible for late and prolonged pseudoprogression.

A few limitations of our study need to be discussed. Due to the retrospective character of the present study, the results need to be confirmed prospectively. Another potential weakness is the relatively small number of patients. On the other hand, we included only IDH-wildtype glioblastoma patients, and this homogenous group of patients was balanced in terms of resection extent and gender distribution. Note that a neuropathological validation was not available for all lesions, and in most lesions, clinicoradiological criteria had to be used for the definite diagnosis. Nevertheless, due to a poor clinical condition or refusal of the patient, another biopsy or surgery could not always be performed.

It should be noted that advanced MRI techniques such as perfusion- and diffusion-weighted MRI as well as proton MR spectroscopy are also of clinical value for the differentiation of tumor progression from pseudoprogression (13). In the recent years, methods from the field of artificial intelligence such as feature-based radiomics are increasingly used for the diagnosis of pseudoprogression. Available study results, mainly based on both conventional and advanced MRI radiomics, are promising (54). Moreover, initial studies evaluating feature-based radiomics computed from FET PET and FET PET evaluation methods based on machine learning suggested also an improvement of diagnostics (55,56).

In summary, our study suggests that FET-PET is of significant clinical value for diagnosing late and prolonged pseudoprogression following lomustine-temozolomide chemoradiation according to the CeTeG/NOA-09 trial. An incorrect diagnosis of tumor progression (i.e., overlooking pseudoprogression) implies that an effective treatment may be erroneously terminated, with a potentially harmful influence on survival. The latter is of particular relevance because treatment options after lomustine-temozolomide chemoradiation are limited, as alkylating agents are usually exhausted. Therefore, additional FET PET imaging should be considered in patients with glioblastoma treated with radiation and intensified alkylating chemotherapy in the case of equivocal MRI findings.

ACKNOWLEDGEMENTS

The Cologne Clinician Scientist-Program (CCSP) of the Deutsche Forschungsgemeinschaft (DFG, FI773/15-1), Germany, supported this work.

REFERENCES

- 1. Stupp R, Mason WP, van den Bent MJ, Weller M, Fisher B, Taphoorn MJ, et al. Radiotherapy plus concomitant and adjuvant temozolomide for glioblastoma. *N* Engl J Med 2005;**352**(10):987-96 doi 10.1056/NEJMoa043330.
- 2. Weller M, Butowski N, Tran DD, Recht LD, Lim M, Hirte H, et al. Rindopepimut with temozolomide for patients with newly diagnosed, EGFRvIII-expressing glioblastoma (ACT IV): a randomised, double-blind, international phase 3 trial. *Lancet Oncol* 2017;**18**(10):1373-85.
- 3. Hegi ME, Diserens AC, Gorlia T, Hamou MF, de Tribolet N, Weller M, et al. MGMT gene silencing and benefit from temozolomide in glioblastoma. *N Engl J Med* 2005;**352**:997-1003.
- 4. Gerson SL. MGMT: its role in cancer aetiology and cancer therapeutics. *Nat Rev Cancer* 2004;**4**(4):296-307 doi 10.1038/nrc1319.
- 5. Herrlinger U, Tzaridis T, Mack F, Steinbach JP, Schlegel U, Sabel M, et al. Lomustine-temozolomide combination therapy versus standard temozolomide therapy in patients with newly diagnosed glioblastoma with methylated MGMT promoter (CeTeG/NOA-09): a randomised, open-label, phase 3 trial. *Lancet* 2019;393(10172):678-88 doi 10.1016/S0140-6736(18)31791-4.
- 6. Stuplich M, Hadizadeh DR, Kuchelmeister K, Scorzin J, Filss C, Langen KJ, *et al.* Late and prolonged pseudoprogression in glioblastoma after treatment with lomustine and temozolomide. *J Clin Oncol* 2012;**30**(21):e180-3.

- 7. Wen PY, Macdonald DR, Reardon DA, Cloughesy TF, Sorensen AG, Galanis E, et al. Updated response assessment criteria for high-grade gliomas: response assessment in neuro-oncology working group. *J Clin Oncol* 2010;**28**(11):1963-72.
- 8. Brandsma D, Stalpers L, Taal W, Sminia P, van den Bent MJ. Clinical features, mechanisms, and management of pseudoprogression in malignant gliomas. *Lancet Oncol* 2008;**9**(5):453-61.
- 9. Brandes AA, Franceschi E, Tosoni A, Blatt V, Pession A, Tallini G, et al. MGMT promoter methylation status can predict the incidence and outcome of pseudoprogression after concomitant radiochemotherapy in newly diagnosed glioblastoma patients. *J Clin Oncol* 2008;**26**(13):2192-7 doi 10.1200/JCO.2007.14.8163.
- 10. Chinot OL, Wick W, Mason W, Henriksson R, Saran F, Nishikawa R, et al. Bevacizumab plus radiotherapy-temozolomide for newly diagnosed glioblastoma. *N* Engl J Med 2014;**370**(8):709-22.
- 11. Balana C, Capellades J, Pineda E, Estival A, Puig J, Domenech S, et al. Pseudoprogression as an adverse event of glioblastoma therapy. *Cancer Med* 2017;**6**(12):2858-66 doi 10.1002/cam4.1242.
- 12. Kumar AJ, Leeds NE, Fuller GN, Van Tassel P, Maor MH, Sawaya RE, et al. Malignant gliomas: MR imaging spectrum of radiation therapy- and chemotherapy-induced necrosis of the brain after treatment. *Radiology* 2000;**217**(2):377-84.
- 13. Langen KJ, Galldiks N, Hattingen E, Shah NJ. Advances in neuro-oncology imaging. *Nat Rev Neurol* 2017;**13**(5):279-89.

- 14. Thust SC, van den Bent MJ, Smits M. Pseudoprogression of brain tumors. *J Magn Reson Imaging* 2018;**48**(3):571-89 doi 10.1002/jmri.26171.
- 15. Galldiks N, Kocher M, Ceccon G, Werner JM, Brunn A, Deckert M, et al. Imaging challenges of immunotherapy and targeted therapy in patients with brain metastases: response, progression, and pseudoprogression. *Neuro Oncol* 2020;**22**(1):17-30 doi 10.1093/neuonc/noz147.
- 16. Galldiks N, Abdulla DS, Scheffler M, Wolpert F, Werner JM, Huellner MW, et al. Treatment Monitoring of Immunotherapy and Targeted Therapy using (18)F-FET PET in Patients with Melanoma and Lung Cancer Brain Metastases: Initial Experiences. *J Nucl Med* 2020 doi 10.2967/jnumed.120.248278.
- 17. Schwarzenberg J, Czernin J, Cloughesy TF, Ellingson BM, Pope WB, Grogan T, et al. Treatment Response Evaluation Using 18F-FDOPA PET in Patients with Recurrent Malignant Glioma on Bevacizumab Therapy. *Clin Cancer Res* 2014;**20**(13):3550-9 doi 10.1158/1078-0432.CCR-13-1440.
- 18. Galldiks N, Dunkl V, Stoffels G, Hutterer M, Rapp M, Sabel M, et al. Diagnosis of pseudoprogression in patients with glioblastoma using O-(2-[18F]fluoroethyl)-L-tyrosine PET. Eur J Nucl Med Mol Imaging 2015;42(5):685-95.
- 19. Werner JM, Stoffels G, Lichtenstein T, Borggrefe J, Lohmann P, Ceccon G, et al. Differentiation of treatment-related changes from tumour progression: a direct comparison between dynamic FET PET and ADC values obtained from DWI MRI. Eur J Nucl Med Mol Imaging 2019;46(9):1889-901 doi 10.1007/s00259-019-04384-7.

- 20. Kebir S, Fimmers R, Galldiks N, Schafer N, Mack F, Schaub C, et al. Late Pseudoprogression in Glioblastoma: Diagnostic Value of Dynamic O-(2-[18F]fluoroethyl)-L-Tyrosine PET. Clin Cancer Res 2016;22(9):2190-6.
- 21. Kertels O, Mihovilovic MI, Linsenmann T, Kessler AF, Tran-Gia J, Kircher M, et al. Clinical Utility of Different Approaches for Detection of Late Pseudoprogression in Glioblastoma With O-(2-[18F]Fluoroethyl)-L-Tyrosine PET. Clin Nucl Med 2019;44(9):695-701 doi 10.1097/RLU.00000000000002652.
- 22. Mihovilovic MI, Kertels O, Hanscheid H, Lohr M, Monoranu CM, Kleinlein I, et al. O-(2-((18)F)fluoroethyl)-L-tyrosine PET for the differentiation of tumour recurrence from late pseudoprogression in glioblastoma. *J Neurol Neurosurg Psychiatry* 2019;**90**(2):238-9 doi 10.1136/jnnp-2017-317155.
- 23. Bashir A, Mathilde Jacobsen S, Molby Henriksen O, Broholm H, Urup T, Grunnet K, et al. Recurrent glioblastoma versus late posttreatment changes: O-(2-[18F]fluoroethyl)-L-tyrosine diagnostic accuracy of positron emission tomography (18F-FET PET). Neuro Oncol 2019;**21**(12):1595-606 doi 10.1093/neuonc/noz166.
- 24. Albert NL, Weller M, Suchorska B, Galldiks N, Soffietti R, Kim MM, et al. Response Assessment in Neuro-Oncology working group and European Association for Neuro-Oncology recommendations for the clinical use of PET imaging in gliomas. *Neuro Oncol* 2016;**18**(9):1199-208.
- 25. Galldiks N, Langen KJ, Albert NL, Chamberlain M, Soffietti R, Kim MM, et al. PET imaging in patients with brain metastasis-report of the RANO/PET group. *Neuro Oncol* 2019;**21**(5):585-95.

- 26. Langen KJ, Stoffels G, Filss C, Heinzel A, Stegmayr C, Lohmann P, et al. Imaging of amino acid transport in brain tumours: Positron emission tomography with O-(2-[(18)F]fluoroethyl)-L-tyrosine (FET). *Methods* 2017;**130**:124-34 doi 10.1016/j.ymeth.2017.05.019.
- 27. Habermeier A, Graf J, Sandhofer BF, Boissel JP, Roesch F, Closs EI. System L amino acid transporter LAT1 accumulates O-(2-fluoroethyl)-L-tyrosine (FET). *Amino Acids* 2015;**47**(2):335-44.
- 28. Melguizo-Gavilanes I, Bruner JM, Guha-Thakurta N, Hess KR, Puduvalli VK. Characterization of pseudoprogression in patients with glioblastoma: is histology the gold standard? *J Neurooncol* 2015;**123**(1):141-50 doi 10.1007/s11060-015-1774-5.
- 29. Young RJ, Gupta A, Shah AD, Graber JJ, Zhang Z, Shi W, et al. Potential utility of conventional MRI signs in diagnosing pseudoprogression in glioblastoma. *Neurology* 2011;**76**(22):1918-24.
- 30. Ellingson BM, Bendszus M, Boxerman J, Barboriak D, Erickson BJ, Smits M, et al. Consensus recommendations for a standardized Brain Tumor Imaging Protocol in clinical trials. *Neuro Oncol* 2015;**17**(9):1188-98 doi 10.1093/neuonc/nov095.
- 31. Hamacher K, Coenen HH. Efficient routine production of the 18F-labelled amino acid O-2-18F fluoroethyl-L-tyrosine. *Appl Radiat Isot* 2002;**57**(6):853-6.
- 32. Law I, Albert NL, Arbizu J, Boellaard R, Drzezga A, Galldiks N, et al. Joint EANM/EANO/RANO practice guidelines/SNMMI procedure standards for imaging of gliomas using PET with radiolabelled amino acids and [(18)F]FDG: version 1.0. Eur J Nucl Med Mol Imaging 2019;46(3):540-57.

- 33. Herzog H, Langen KJ, Weirich C, Rota Kops E, Kaffanke J, Tellmann L, et al. High resolution BrainPET combined with simultaneous MRI. *Nuklearmedizin* 2011;**50**(2):74-82.
- 34. Lohmann P, Herzog H, Rota Kops E, Stoffels G, Judov N, Filss C, *et al.* Dual-time-point O-(2-[(18)F]fluoroethyl)-L-tyrosine PET for grading of cerebral gliomas. *Eur Radiol* 2015;**25**(10):3017-24.
- 35. Rapp M, Heinzel A, Galldiks N, Stoffels G, Felsberg J, Ewelt C, et al. Diagnostic performance of 18F-FET PET in newly diagnosed cerebral lesions suggestive of glioma. *J Nucl Med* 2013;**54**(2):229-35.
- 36. Pauleit D, Floeth F, Hamacher K, Riemenschneider MJ, Reifenberger G, Müller HW, et al. O-(2-[18F]fluoroethyl)-L-tyrosine PET combined with MRI improves the diagnostic assessment of cerebral gliomas. *Brain* 2005;**128**(3):678-87.
- 37. Galldiks N, Stoffels G, Filss C, Rapp M, Blau T, Tscherpel C, et al. The use of dynamic O-(2-18F-fluoroethyl)-I-tyrosine PET in the diagnosis of patients with progressive and recurrent glioma. *Neuro Oncol* 2015;**17**(9):1293-300.
- 38. Galldiks N, Langen KJ, Holy R, Pinkawa M, Stoffels G, Nolte KW, et al. Assessment of treatment response in patients with glioblastoma using O-(2-18F-fluoroethyl)-L-tyrosine PET in comparison to MRI. *J Nucl Med* 2012;**53**(7):1048-57 doi 10.2967/jnumed.111.098590.
- 39. Bauer EK, Stoffels G, Blau T, Reifenberger G, Felsberg J, Werner JM, et al. Prediction of survival in patients with IDH-wildtype astrocytic gliomas using dynamic O-(2-[(18)F]-fluoroethyl)-L-tyrosine PET. *Eur J Nucl Med Mol Imaging* 2020;**47**(6):1486-95 doi 10.1007/s00259-020-04695-0.

- 40. Louis DN, Perry A, Reifenberger G, von Deimling A, Figarella-Branger D, Cavenee WK, et al. The 2016 World Health Organization Classification of Tumors of the Central Nervous System: a summary. *Acta Neuropathol* 2016;**131**(6):803-20.
- 41. Capper D, Weissert S, Balss J, Habel A, Meyer J, Jager D, et al. Characterization of R132H mutation-specific IDH1 antibody binding in brain tumors.

 Brain pathology 2010;20(1):245-54.
- 42. Hartmann C, Hentschel B, Wick W, Capper D, Felsberg J, Simon M, et al. Patients with IDH1 wild type anaplastic astrocytomas exhibit worse prognosis than IDH1-mutated glioblastomas, and IDH1 mutation status accounts for the unfavorable prognostic effect of higher age: implications for classification of gliomas. *Acta Neuropathol* 2010;**120**:707-18.
- 43. Felsberg J, Rapp M, Loeser S, Fimmers R, Stummer W, Goeppert M, et al. Prognostic significance of molecular markers and extent of resection in primary glioblastoma patients. *Clin Cancer Res* 2009;**15**:6683-93.
- 44. Yokogami K, Yamasaki K, Matsumoto F, Yamashita S, Saito K, Tacheva A, et al. Impact of PCR-based molecular analysis in daily diagnosis for the patient with gliomas. *Brain Tumor Pathol* 2018;**35**(3):141-7.
- 45. Radbruch A, Lutz K, Wiestler B, Baumer P, Heiland S, Wick W, et al. Relevance of T2 signal changes in the assessment of progression of glioblastoma according to the Response Assessment in Neurooncology criteria. *Neuro Oncol* 2012;**14**(2):222-9 doi 10.1093/neuonc/nor200.

- 46. Pyka T, Hiob D, Preibisch C, Gempt J, Wiestler B, Schlegel J, et al. Diagnosis of glioma recurrence using multiparametric dynamic 18F-fluoroethyl-tyrosine PET-MRI. Eur J Radiol 2018;**103**:32-7 doi 10.1016/j.ejrad.2018.04.003.
- 47. Radbruch A, Fladt J, Kickingereder P, Wiestler B, Nowosielski M, Baumer P, et al. Pseudoprogression in patients with glioblastoma: clinical relevance despite low incidence. *Neuro Oncol* 2015;**17**(1):151-9 doi 10.1093/neuonc/nou129.
- 48. Li H, Li J, Cheng G, Zhang J, Li X. IDH mutation and MGMT promoter methylation are associated with the pseudoprogression and improved prognosis of glioblastoma multiforme patients who have undergone concurrent and adjuvant temozolomide-based chemoradiotherapy. *Clin Neurol Neurosurg* 2016;**151**:31-6 doi 10.1016/j.clineuro.2016.10.004.
- 49. Kong DS, Kim ST, Kim EH, Lim DH, Kim WS, Suh YL, *et al.* Diagnostic dilemma of pseudoprogression in the treatment of newly diagnosed glioblastomas: the role of assessing relative cerebral blood flow volume and oxygen-6-methylguanine-DNA methyltransferase promoter methylation status. *AJNR Am J Neuroradiol* 2011;**32**(2):382-7 doi 10.3174/ajnr.A2286.
- 50. Hygino da Cruz LC, Jr., Rodriguez I, Domingues RC, Gasparetto EL, Sorensen AG. Pseudoprogression and pseudoresponse: imaging challenges in the assessment of posttreatment glioma. *AJNR Am J Neuroradiol* 2011;**32**:1978-85.
- 51. Chaskis C, Neyns B, Michotte A, De Ridder M, Everaert H. Pseudoprogression after radiotherapy with concurrent temozolomide for high-grade glioma: clinical observations and working recommendations. *Surg Neurol* 2009;**72**(4):423-8 doi 10.1016/j.surneu.2008.09.023.

- 52. Chamberlain MC, Glantz MJ, Chalmers L, Van Horn A, Sloan AE. Early necrosis following concurrent Temodar and radiotherapy in patients with glioblastoma. *J Neurooncol* 2007;**82**(1):81-3 doi 10.1007/s11060-006-9241-y.
- 53. Peyre M, Cartalat-Carel S, Meyronet D, Ricard D, Jouvet A, Pallud J, et al. Prolonged response without prolonged chemotherapy: a lesson from PCV chemotherapy in low-grade gliomas. *Neuro Oncol* 2010;**12**(10):1078-82 doi 10.1093/neuonc/noq055.
- 54. Elshafeey N, Kotrotsou A, Hassan A, Elshafei N, Hassan I, Ahmed S, et al. Multicenter study demonstrates radiomic features derived from magnetic resonance perfusion images identify pseudoprogression in glioblastoma. *Nat Commun* 2019;**10**(1):3170 doi 10.1038/s41467-019-11007-0.
- 55. Lohmann P, Elahmadawy MA, Gutsche R, Werner JM, Bauer EK, Ceccon G, et al. FET PET Radiomics for Differentiating Pseudoprogression from Early Tumor Progression in Glioma Patients Post-Chemoradiation. *Cancers (Basel)* 2020;**12**(12) doi 10.3390/cancers12123835.
- 56. Kebir S, Schmidt T, Weber M, Lazaridis L, Galldiks N, Langen KJ, et al. A Preliminary Study on Machine Learning-Based Evaluation of Static and Dynamic FET-PET for the Detection of Pseudoprogression in Patients with IDH-Wildtype Glioblastoma. *Cancers (Basel)* 2020;**12**(11) doi 10.3390/cancers12113080.

Table 1: Overview of clinical data

#	Gender, age (years) at initial diagnosis	EoR	Number of LOM-TMZ cycles before suspicious MRI	Weeks between radiotherapy completion and suspicious MRI	Suspicious MRI findings	
1	F, 63	PR	3	8	enlargement of T2 or FLAIR hyperintensity > 15%	
2	M, 62	PR	3	8	enlargement of CE ≥ 25%	
3	F, 70	В	3	7	enlargement of CE ≥ 25%	
4	F, 46	PR	3	9	enlargement of CE < 25%	
5	F, 47	CR	6	30	new CE	
6	M, 59	В	3	9	enlargement of CE ≥ 25%	
7	F, 45	CR	3	9	new CE	
8	M, 65	CR	5	28	new CE	
9	F, 60	CR	3	14	enlargement of CE ≥ 25%	
10	M, 70	CR	5	25	enlargement of T2 or FLAIR hyperintensity > 15%	
11	M, 67	CR	3	25	enlargement of T2 or FLAIR hyperintensity > 15%	
12	F, 60	В	3	16	enlargement of CE < 25%	
13	F, 64	PR	2	5	enlargement of CE ≥ 25%	
14	M, 59	PR	3	10	new CE	
15	M, 55	PR	4	24	new CE	
16	F, 67	PR	2	5	new CE, diameter < 10 mm	
17	M, 37	CR	3	10	enlargement of CE ≥ 25%	
18	M, 50	В	3	10	enlargement of CE < 25%	
19	M, 66	PR	4	11	enlargement of CE < 25%	
20	M, 50	CR	2	9	enlargement of CE ≥ 25%	
21	F, 49	CR	3	8	new CE	
22	M, 48	CR	4	16	new CE	
23	M, 62	CR	6	34	new CE	

Abbreviations: B = stereotactic biopsy; **CE** = contrast-enhancing lesion; **CR** = complete resection; **EoR** = extent of resection; **F** = female; **LOM-TMZ** = lomustine-temozolomide chemotherapy; **M** = male; **PR** = partial resection

Table 2: PET imaging results

#	TBR _{mean}	TBR _{max}	TTP (minutes)	Slope (SUV/h)	Baseline/ follow-up PET	Diagnosis	Confirmation of diagnosis	Onset of pseudoprogression after completion of radiotherapy (weeks)	Begin of MRI improvement after pseudoprogression onset (weeks)
1	2.0	2.9	27.5	0.01	yes	TP	clinicorad	-	-
2	1.8	2.3	22.5	-0.04	yes	pseudoprogression	neuropathologically	8	n.a.
3	2.2	3.5	32.5	-0.62	yes	pseudoprogression	clinicorad	7	35
4	1.9	3.0	47.5	0.62	yes	pseudoprogression	clinicorad	9	30
5	2.2	3.4	27.5	0.60	no	TP	clinicorad	-	-
6	2.4	4.4	37.5	0.11	yes	pseudoprogression	clinicorad	9	30
7	1.7	2.3	42.5	0.52	yes	pseudoprogression	clinicorad	9	52
8	2.1	4.2	15.5	-0.47	no	TP	neuropathologically	-	-
9	1.9	2.9	37.5	0.70	no	pseudoprogression	neuropathologically	14	66
10	2.0	2.9	12.5	-0.67	no	TP	clinicorad	-	-
11	1.8	2.6	37.5	0.23	no	pseudoprogression	clinicorad	25	34
12	1.7	2.0	32.5	-0.05	no	TP	clinicorad	-	-
13	1.8	2.2	27.5	0.03	no	pseudoprogression	clinicorad	5	n.a.
14	2.1	3.7	18.5	-0.49	no	TP	clinicorad	-	-
15	2.0	3.3	27.5	-0.02	no	TP	neuropathologically	-	-
16	2.0	2.9	32.5	0.11	no	TP	clinicorad	-	-
17	2.0	3.2	12.5	-0.59	no	TP	neuropathologically	-	-
18	1.8	2.8	27.5	-0.38	no	pseudoprogression	clinicorad	10	99
19	2.0	3.4	15.5	-0.20	no	TP	clinicorad	-	-
20	1.9	2.6	42.5	0.36	no	pseudoprogression	clinicorad	9	n.a.
21	1.9	2.5	47.5	0.64	yes	pseudoprogression	clinicorad	8	26
22	2.2	3.6	37.5	0.58	yes	TP	neuropathologically	-	-
23	2.4	3.7	37.5	-0.03	no	TP	clinicorad	-	-

Abbreviations: clinicorad = clinicoradiological confirmation of diagnosis; **n.a.** = not available; **SUV** = standardized uptake value; **TBR**_{mean} = mean tumor-to-brain ratio of FET PET uptake; **TBR**_{max} = maximum tumor-to-brain ratio of FET PET; **TTP** = time-to-peak; **TP** = tumor progression

Table 3: Diagnostic performance of static and dynamic FET PET parameters

	TBR _{mean}	TBR _{max}	Slope	TTP	Combined analysis of TBR _{mean} and TTP	Combined analysis of TBR _{max} and TTP
Threshold for the identification of pseudoprogression	< 1.95	< 2.85	> 0.02 SUV/h	> 35 minutes	TBR _{mean} < 1.95 and TTP > 35 minutes	TBR _{max} < 2.85 and TTP > 35 minutes
Sensitivity (%)	82	64	73	64	55	36
Specificity (%)	92	92	75	83	100	100
Diagnostic accuracy (%)	87	78	74	74	78	70
Positive predictive value (%)	90	88	73	78	100	100
Negative predictive value (%)	85	73	75	71	71	63
AUC ± standard error	0.77 ± 0.12	0.75 ± 0.11	0.72 ± 0.11	0.82 ± 0.09	n.a.	n.a.
<i>P</i> -value	0.029	0.046	0.069	0.010	0.005	0.037

Abbreviations: AUC = area under the receiver operating characteristic curve; **n.a.** = not available; **SUV** = standardized uptake value; TBR_{max} = maximal tumor-to-brain ratio of FET uptake; TBR_{mean} = mean tumor-to-brain ratio of FET uptake; TP = time-to-peak

FIGURE LEGENDS

Figure 1: Contrast-enhanced MRI and FET PET of a 70-year-old female patient with a newly diagnosed glioblastoma (IDH-wildtype, MGMT promoter methylated) treated with lomustine-temozolomide chemoradiation. After completing radiotherapy, the contrast-enhancing lesion progressed from week 7 to week 29 (top row). In contrast, relative to the baseline scan, follow-up FET-PET scans at weeks 7 and 15 showed a decreased metabolic activity of 13% (i.e., a relative reduction of mean tumor-to-brain ratios) and indicated pseudoprogression (bottom row). Without clinical deterioration or change of treatment, the patient had completed 6 cycles of lomustine-temozolomide chemotherapy. From week 42 to week 94, the contrast-enhancing lesion on MRI regressed completely (top row). The corresponding time-activity curves are provided in Supplemental Figure 1.

Figure 2: MR images and FET PET of a 61-year-old female patient with a newly diagnosed glioblastoma (IDH-wildtype, MGMT promoter methylated) treated with lomustine and temozolomide chemoradiation. Fourteen weeks after radiotherapy, contrast-enhanced and FLAIR-weighted MRI suggested tumor progression (middle column). In contrast, FET PET revealed no pathologically increased metabolic activity (bottom left). The combination of static and dynamic FET parameters calculated from the time-activity curve (bottom right) suggested pseudoprogression. The histology of tissue samples obtained from stereotactic biopsy revealed necrotic changes (A), hyalinized and thickened vessels (A, arrows) indicating actinic angiopathy (hematoxylin and eosin stain), resorptive tissue, mainly composed of CD68-positive macrophages (B), and intermingled CD3-positive (C) and CD8-positive T-lymphocytes (C, insert) without vital tumor tissue (original magnification, 200x; scale bar, 100 μm). In summary, neuropathological findings were consistent with

pseudoprogression. Subsequently, the patient was in a stable clinical condition for 22 months until a local tumor progression and a distant tumor relapse prompted treatment change.

Figure 1

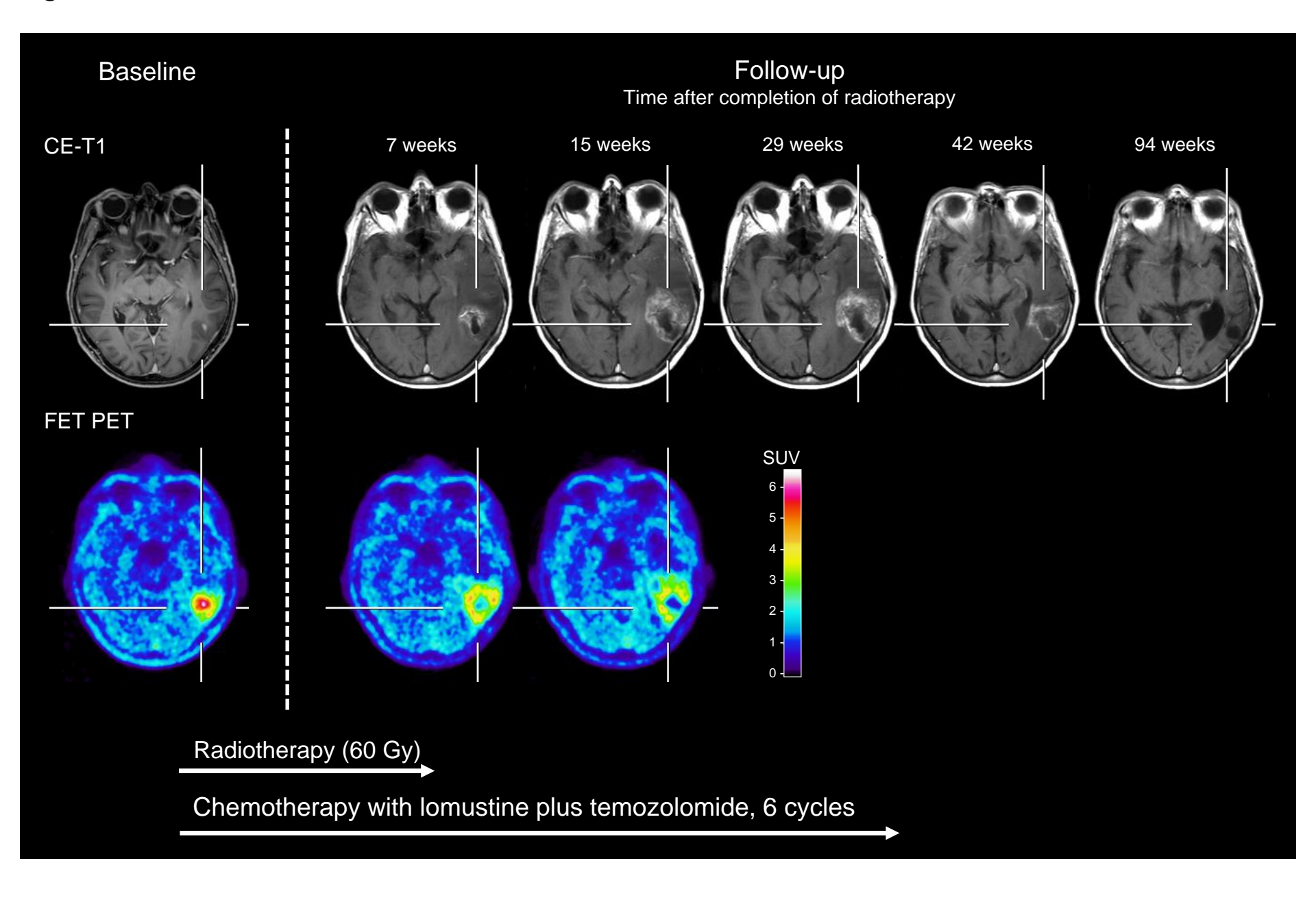


Figure 2

